Lipid Domains in Bicelles Containing Unsaturated Lipids and Cholesterol

Hyo Soon Cho, Johnna L. Dominick, and Megan M. Spence*

Chevron Science Center, Department of Chemistry, University of Pittsburgh, Pittsburgh, Pennsylvania 15260

Received: January 11, 2010; Revised Manuscript Received: May 15, 2010

We have created a stable bicelle system capable of forming micrometer-scale lipid domains that orient in a magnetic field, suitable for structural biology determination in solid-state NMR. The bicelles consisted of a mixture of cholesterol, saturated lipid (DMPC), and unsaturated lipid (POPC), a mixture commonly used to create domains in model membranes, along with a short chain lipid (DHPC) that allows formation of the bicelle phase. While maintaining a constant molar ratio of long to short chain lipids, $q = ([POPC]+[DMPC])/[DHPC] = 3$, we varied the concentrations of the unsaturated lipid, POPC, and cholesterol to observe the effects of the components on bicelle stability. Using ^{31}P solid-state NMR, we observed that unsaturated lipids (POPC) greatly destabilized the alignment of the membranes in the magnetic field, while cholesterol stabilized their alignment. By combining cholesterol and unsaturated lipids in the bicelles, we created membranes aligning uniformly in the magnetic field, despite very high concentrations of unsaturated lipids. These bicelles, with high concentrations of both cholesterol and unsaturated lipid, showed similar phase behavior to bicelles commonly used in structural biology, but aligned over a wider temperature range (291−314 K). Domains were observed by measuring time-dependent diffusion constants reflecting restricted diffusion of the lipids within micrometer-scale regions of the bicelles. Micron-scale domains have never been observed in POPC/DMPC/cholesterol vesicles, implying that bilayers in bicelles show different phase behavior than their counterparts in vesicles, and that bilayers in bicelles favor domain formation.

1. Introduction

Membrane rafts are hypothesized to organize the cell membrane by creating a lateral phase separation of lipids capable of sorting membrane proteins and regulating their activity.[1] Lipid domains have been demonstrated in model membranes formed from a ternary mixture consisting of the following components: unsaturated lipids, saturated lipids, and cholesterol, and are considered a model system for membrane rafts. On the basis of model membranes, membrane rafts are described as in the liquid ordered (l_o) state, and show distinctly different structural and dynamical properties than the liquid disordered (l_d) state common in cellular membranes. These structural and dynamical differences are important to the function of membrane rafts in modulating protein structure and accessibility,[2] but molecular details of the interaction between rafts and proteins are lacking.

Model membranes containing lipid domains have not been used for membrane protein structural biology, mainly because of the severe constraints that the techniques place on the membrane composition. X-ray crystallography of membrane proteins employs detergents to solvate hydrophobic regions of the protein, or use 3D crystals of lipid bilayers.[3] Solid-state NMR can use intact lipid bilayers, but many experiments are designed for uniaxially aligned membrane samples, either mechanically aligned between glass slips, or aligned in the magnetic field.[4] The alignment of these membranes is very sensitive to membrane composition, and has been optimized for membranes composed of saturated phosphatidylcholines. For example, when the molar ratio of short and long chain lipid is altered, the bilayer structure and its alignment are varied.[5]

The molecular composition of the membrane affects structural properties like membrane thickness and flexibility,[6] dynamic properties like membrane fluidity,[7] and the formation of phases like lipid rafts.[8−10] Hydrophobic matching and membrane thickness can affect the activity of membrane proteins[11,12] and membrane composition can modulate membrane protein function.[13−15] Cholesterol has been shown to control the structural interactions between some antimicrobial peptides and membranes.[16] Lipid rafts are thought to be thicker than the surrounding membrane[17] and show slower lipid diffusion in measurements of model membranes,[18] but the effect of these membrane structural differences on protein structure has not been studied and is unknown.

Bicelles are model membranes well suited to magnetic resonance studies of membrane protein structure because of their ability to orient in a magnetic field,[19] and have been used in most NMR structural studies of transmembrane proteins.[4,20−26] However, like most model membranes, bicelles usually consist solely of saturated chain phosphatidylcholines, with a long chain lipid forming the bilayer and a short chain lipid solvating any perforations in the bilayer. Bicelles have been created with unsaturated lipids,[27,28] cardiolipin,[29,30] and cholesterol,[27,31,32] but the stability decreased as the fraction of saturated lipids decreased. Unfortunately, the stability and alignment of the bicelles can be greatly affected by even a small change in the membrane composition.[24,27,28,33] ^{31}P NMR can monitor any changes in the morphology of the bicelles caused by the addition of new membrane components, and can measure the stability and alignment of bicelle systems.

Lateral diffusion of lipids is a useful metric of the state of a lipid bilayer,[34] and is sensitive to parameters like lipid composition, cholesterol content, and temperature. Pulsed field gradient (PFG) NMR is a well-established tool for measuring the self-diffusion constant of lipids in bilayers, relying on magic angle spinning (MAS)[35] or macroscopic orientation of the bilayers at the magic angle[36] to narrow the ^{1}H signals characteristic of

* To whom correspondence should be addressed. E-mail: mspence@pitt.edu.

10.1021/jp100276u
Published on Web 06/28/2010

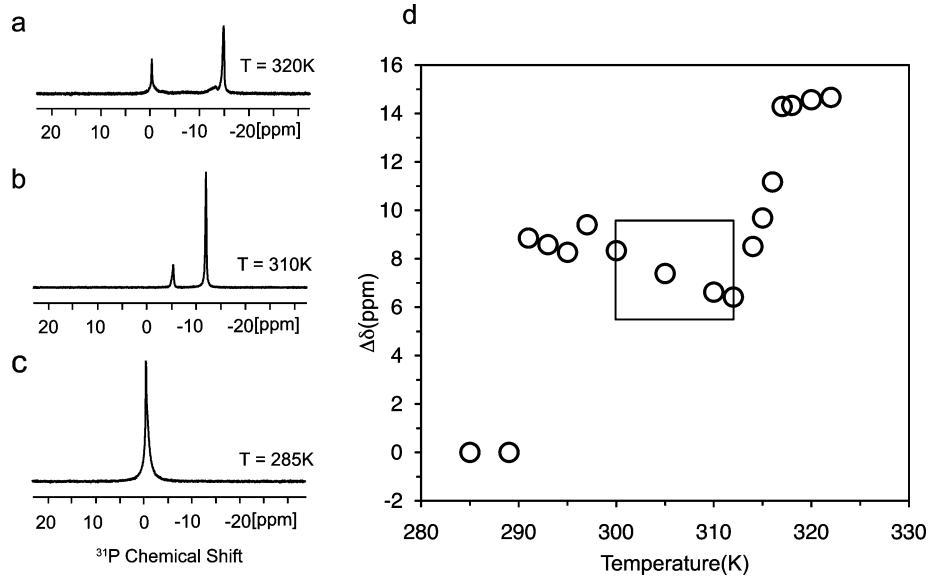

Figure 1. ^{31}P chemical shift difference ($\triangle\delta$) as a measure of bicelle phase. Parts (a)−(c) Vesicle, bicelle, and gel spectra, respectively, of 3.5/1 DMPC/DHPC conventional bicelles. (d) Chemical shift difference increases from 0 ppm (gel phase) to ∼8 ppm (aligned bicelles) to ∼15 ppm (vesicles) as temperature of sample is increased. Aligned bicelle phase is present for temperature range defined by box.

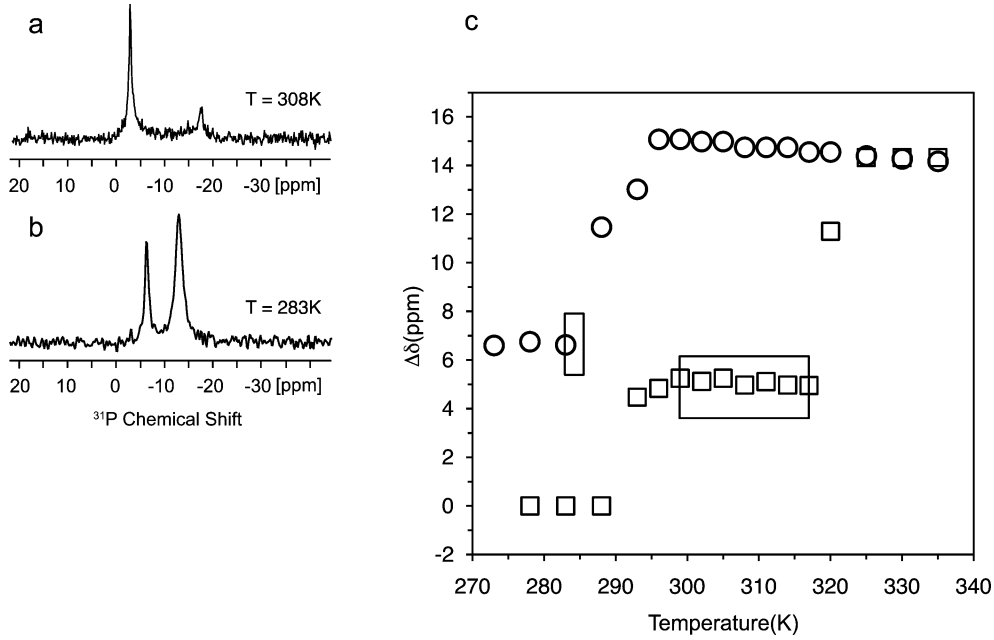

Figure 2. Unsaturated lipids destabilize bicelle alignment. Parts (a),(b) Representative ^{31}P spectra of 1.5/1.5/1 DMPC/POPC/DHPC unsaturated bicelles in vesicle and bicelle phase. (c) 1.5/1.5/1 DMPC/POPC/DHPC bicelles (○) aligned over a small range of ∼5 K due to the loose chain packing of unsaturated acyl chain. In contrast, 2.6/0.4/1 DMPC/POPC/DHPC bicelles (□) behaved similarly to bicelles without any unsaturated lipids.

anisotropic molecular systems. Using PFG NMR, distinct diffusion constants have been observed for lipids in the l_o and l_d phases, and the onset of domain formation has been measured for domain forming systems.[18,37,38] The size of lipid domains has been measured by using PFG NMR experiments to observe the lipid diffusion behavior as a function of diffusion time, with the time-dependent diffusion constant offering a measure of the length scale of membrane inhomogeneity.[39,40]

2. Experimental Section

2.1. Sample Preparation. 1,2-dimyristoyl-*sn*-glycero-3-phosphatidylcholine (DMPC, 99%) in powder form, 1,2-dihexanoyl-*sn*-glycero-3-phosphatidylcholine (DHPC, 99%) in chloroform, and 1-palmitoyl-2-oleoyl-*sn*-glycero-3-phosphatidylcholine (POPC) in chloroform were purchased from Avanti Polar Lipids (Birmingham, AL). Lipids were used as purchased without further purification. Cholesterol (ovine wool, >98%) in powder form, 4-(2-hydroxyethyl)-1-piperazineethanesulfonic acid (HEPES, ≥99.5%) and sodium azide were purchased from Sigma-Aldrich (Allentown, PA). Deuterium oxide was purchased from Cambridge Isotopes Lab (Woburn, MA).

The lipids were dissolved in chloroform and combined in a molar ratio of 2.6/0.4/1 and 1.5/1.5/1 molar ratios of DMPC/POPC/DHPC with and without 13 mol % cholesterol (calculated with respect to moles of long chain lipids) to create unsaturated

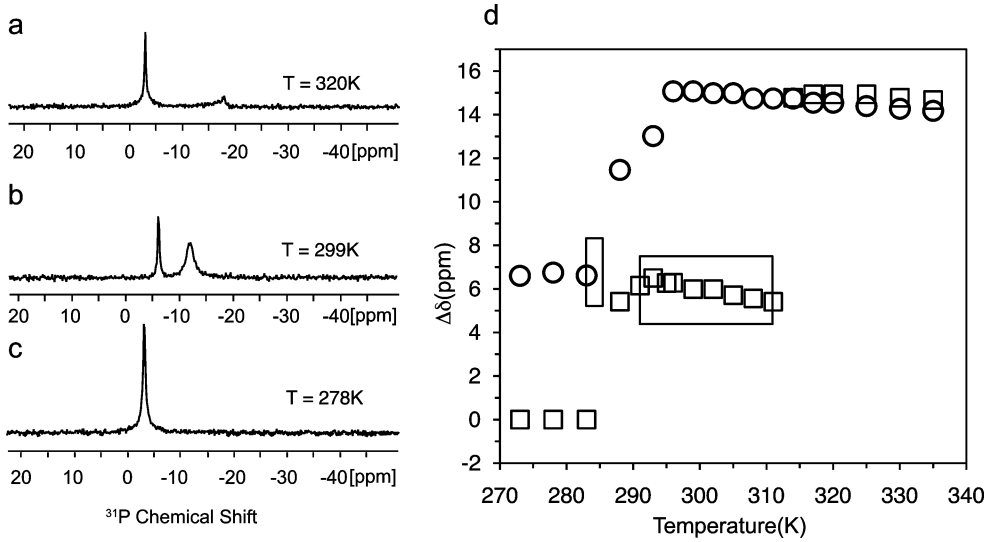

Figure 3. Cholesterol increases alignment temperature range of bicelles. Parts (a)−(c) Representative ^{31}P spectra of 1.5/1.5/1/13 mol % DMPC/POPC/DHPC/cholesterol bicelles in vesicle, bicelle, and gel phase. (d) Bicelles containing unsaturated lipid and cholesterol (□) show increased stability over conventional bicelles and bicelles containing only unsaturated lipid (○) due to condensing effect of cholesterol on the lipid membrane.

TABLE 1: Alignment Behavior of Bicelles Containing Unsaturated Lipids and Cholesterol

[DMPC]/[POPC]/[DHPC]/mol % cholesterol	T_{align} (K)	ΔT_{align} alignment range (K)
3.5/0/1/0 mol % (conventional bicelle)	300	300−314
1.5/1.5/1	283	283−288
1.5/1.5/1/13 mol %	291	291−314
2.6/0.4/1	299	299−320
2.6/0.4/1/13 mol %	317	>325[a]

[a] Temperatures above 325 K were not sampled.

bicelles. A conventional bicelle sample (no cholesterol or unsaturated lipids) was composed of DHPC and DMPC dissolved in chloroform with molar ratio, q = [DMPC]/[DHPC], equal to 3.5. The lipid mixtures were placed under a nitrogen gas flow for ∼20 min to remove chloroform and then placed on a vacuum line for at least 4 h until the sample was reduced to a powder or powder/film mixture. A mixture of 10% deuterium oxide and water was added to each unsaturated bicelle sample to a concentration of 30% w/w. A 20 mM HEPES buffer (pH = 7.1) was used to redissolve the conventional bicelle mixture to a concentration of 30% w/w. Three cycles of the following: heating at 40 °C for 15 min, vortexing for 2 min, cooling at 0 °C for 15 min and again vortexing for 2 min, were performed to form bicelle mixtures.

2.2. NMR Measurements. All spectra were acquired with an 11.7 T magnet with a Bruker Avance console (Bruker Biospin, Billerica, MA) and BCU05 Variable Temperature Control Unit. All sample rotors were 200 μL Bruker 4 mm ZrO_2 magic-angle spinning (MAS) rotors.

A 4-mm HXY MAS probe, was used to acquire the ^{31}P NMR spectra. All ^{31}P experiments were performed under static conditions. The variable temperature ^{31}P experiments at 201.98 MHz used FLOPSY at 6 kHz[41] for proton decoupling. The temperature was varied from 273 to 335 K, in increments of 5 or 3 K with the sample equilibrating in the probe for 10 to 15 min at each temperature. The ^{31}P chemical shifts are referenced to 85% phosphoric acid.

A high-resolution HCN HR-MAS probe (Bruker Biospin, Billerica, MA) was used to acquire the ^{1}H NMR spectra. All

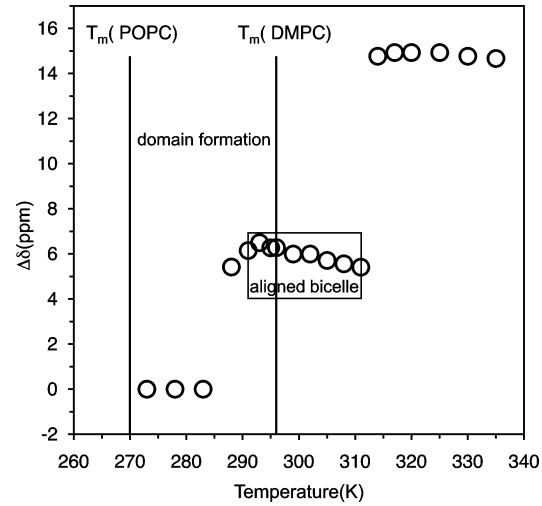

Figure 4. The presence of lipid domains is possible in 1.5/1.5/1/13 mol % molar ratios of DMPC/POPC/DHPC/cholesterol bicelles. Alignment of 1.5/1.5/1/chol DMPC/POPC/DHPC bicelles begins at 291 K, between the two T_m of DMPC (296 K) and POPC (270 K), so domains between 291 and 296 K should orient in magnetic field.

^{1}H experiments were performed under MAS at 5kHz in order to obtain isotropic spectra. ^{1}H spectra were acquired after temperature equilibration for 30 min. ^{1}H diffusion NMR spectra were recorded at 499.81 MHz with a stimulated echo bipolar pulsed field gradient diffusion experiments using WATERGATE for water suppression.[42,43] The maximum gradient strength of the magic angle gradient coil was 0.513 T/m. The intensities of the acyl peak (1.2 ppm) were used to calculate the diffusion coefficient. The ^{1}H chemical shifts are referenced to H_2O.

3. Results and Discussion

3.1. Creating Magnetically Alignable Lipid Domains. ***3.1.1. ^{31}P Spectra As a Metric for Alignment and Phase.*** The ^{31}P chemical shift anisotropy of phospholipids is a sensitive probe of the lipid phase and membrane morphology. Aligned bicelles show a characteristic ^{31}P spectrum with two narrow, symmetric lines (Figure 1b) separated by ∼8 ppm.[44] The chemical shift difference reflects the width of the chemical shift

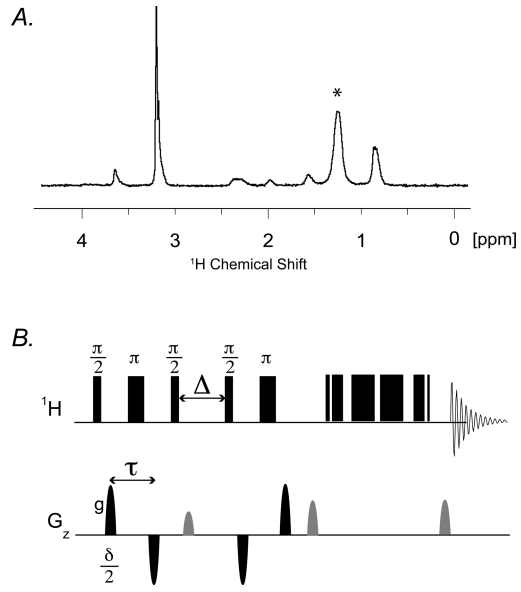

Figure 5. (a) ^{1}H solid-state NMR spectrum of magnetically aligned 1.5/1.5/1/13 mol % DMPC/POPC/DHPC/cholesterol unsaturated bicelles using WATERGATE under magic angle spinning. * acyl peak integrated for diffusion experiment. (b) 1D sequence using stimulated-echo bipolar pulsed field gradient with WATERGATE sequence. During first period, spin positions are encoded along spinning axis by a bipolar gradient pulse of duration $\delta/2$ and amplitude g. This spin magnetization is stored longitudinally during diffusion time, Δ, before the bipolar gradient is applied again.

anisotropy pattern of the phosphatidylcholine headgroup, and the two peaks arise from the different orientations of lipids in the plane of the membrane and the lipids solvating the holes in the membrane. Three ^{31}P spectra of conventional bicelles (q = 3.5) at different temperatures are shown in Figure 1 to mark the different phases of the lipid mixture. To summarize the phase behavior of the lipid mixture, we use the chemical shift difference, $\Delta\delta$, between the upfield and downfield peaks in the spectra. In the gel phase at 285 K, only one ^{31}P peak is present so the chemical shift difference is 0 ppm (Figure 1c). When the bicelles align at 310 K the two peaks are separated by ~8 ppm (Figure 1b) and at 320 K the peaks are approximately 15 ppm apart (Figure 1a), reflecting the transition to vesicles. Plotting $\Delta\delta$ as a function of temperature (Figure 1d) shows the major changes in lipid phase as reflected in the ^{31}P spectrum. The stability and phase behavior of bicelles can be described by the following two parameters: T_{align}, the temperature at which two symmetric peaks appear in the ^{31}P spectrum, and ΔT_{align}, the temperature range over which the bicelles align, indicated by a box in the phase diagram (Figure 1d).

The incorporation of unsaturated lipids or membrane components such as cholesterol increases are necessary for domain formation but can also strongly alter the phase behavior and alignment temperature of a bicelle system. To explore this, we made model membranes containing saturated long chain DMPC and short chain DHPC lipids as well as unsaturated long chain lipid POPC (palmitoyl-2-oleoyl-*sn*-glycero-3-phosphatidylcholine). In addition, in order to look at the effect of cholesterol in the model membrane, we added 13 mol % of cholesterol with respect to long chain lipids into bicelles containing POPC. The phase transitions of the model membranes between different morphologies were detected by solid state ^{31}P NMR spectroscopy and these spectra were used to create phase diagrams like that of Figure 1d.

3.1.2. Effect of Unsaturated Long Chain Lipid on Bicelles. In order to examine the effect of unsaturated long chain lipids on the ability of the membrane to align in the magnetic field, we combined DMPC and DHPC with two different molar amounts of unsaturated lipid. One sample contained a small amount of unsaturated lipid, with molar ratios of 2.6/0.4/1 of DMPC/POPC/DHPC, while another contained equal amounts of saturated and unsaturated long chain lipids (similar to biological membranes[45]), with a 1.5/1.5/1 molar ratio of DMPC/POPC/DHPC. Figure 2a,b shows the ^{31}P NMR spectra of the 1.5/1.5/1 DMPC/POPC/DHPC bicelles at main phase transition temperatures between 270 and 325 K. The spectrum in Figure 2b exhibits the two symmetric lines characteristic of membrane alignment in the magnetic field. The width of the peak at −13.2 ppm likely reflects a distribution in the orientation of the bilayer normal. The spectrum in Figure 2a is consistent with the formation of vesicles above 288 K observed in previous bicelle studies.[5] We also measured ^{31}P NMR spectra of the 2.6/0.4/1 molar ratios of DMPC/POPC/DHPC unsaturated lipid bicelles at temperatures between 273 and 325 K and created phase diagrams of both model membranes (Figure 2c). The 2.6/0.4/1 DMPC/POPC/DHPC bicelles show that small amounts of unsaturated lipid do not significantly change the alignment temperature, T_{align}, or alignment temperature range, ΔT_{align}, of bicelles. However, bicelles containing equal amounts of saturated and unsaturated long chain lipids aligned at a much lower temperature (T_{align} = 283 K) and aligned over a very small temperature range (ΔT_{align} < 5 K). While the large component of unsaturated lipids makes this bicelle system a good model for cellular membranes, the small alignment range makes it a poor model membrane for structural and biophysical studies.

3.1.3. Effect of Cholesterol on Bicelles. In order to look at the effect of cholesterol in the model membrane, we added 13 mol % of cholesterol to both unsaturated bicelle samples, reflecting the cholesterol content of the endoplasmic reticulum.[46] Cholesterol is able to restrict the motion of the lipid chains and increase the lipid membrane stability,[33] possibly counteracting the effect of unsaturated lipid on the alignment of bicelles.[27] Representative ^{31}P NMR spectra of the 1.5/1.5/1/13 mol % DMPC/POPC/DHPC/cholesterol bicelles are shown in Figure 3a−c for main phase transition temperatures between 273 and 325 K. At 278 K, the lipids are in the gel state (Figure 3c), transitioning to aligned bicelles at 291 K (Figure 3b), and to vesicles at 315 K (Figure 3a). As shown before, we created a phase diagram of model membranes containing 1.5/1.5/1 DMPC/POPC/DHPC with and without cholesterol, shown in Figure 3d. In the case of the 1.5/1.5/1 DMPC/POPC/DHPC bicelles, cholesterol increased the alignment temperature, T_{align}, from 283 to 291 K, and increased the ΔT_{align} to 20 K (see Table 1).

Among these model membranes, the 1.5/1.5/1/13 mol % DMPC/POPC/DHPC/cholesterol unsaturated bicelles show the greatest similarity to biological membranes and the greatest stability, reflected in the large alignment temperature range.

3.2. Restricted Diffusion Indicates Lipid Domains. The formation of domains has been noted in many systems combining saturated and unsaturated lipids, arising from the different main chain phase transition temperatures, T_{m}, for the two components.[47] Below the T_{m} of the unsaturated component, the lipids are miscible in the gel state. In the presence of cholesterol, when the sample is heated above the transition temperature for the unsaturated component, the saturated lipids remain in the ordered state, l_o, but the unsaturated chains form domains of liquid-disordered (l_d) phase.[10] Once the sample is heated above the T_{m} for the saturated lipid, both components are in the l_d phase and mix uniformly again. Domains can be present between the transition temperatures of the two components. According

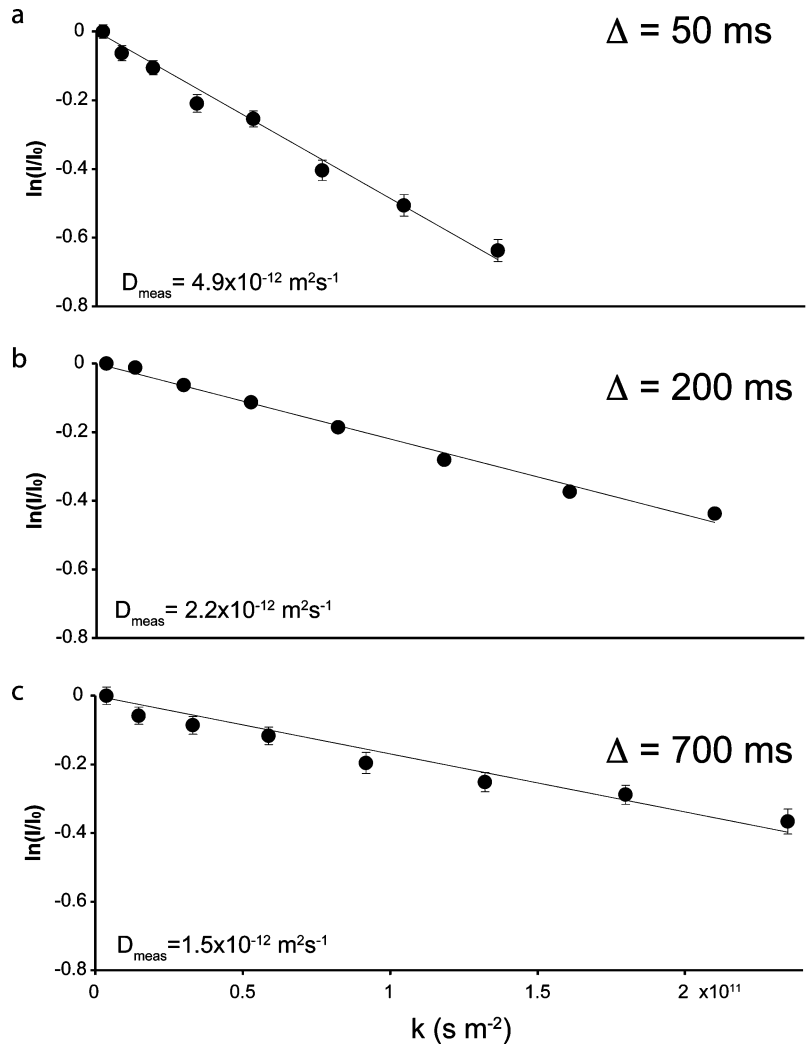

Figure 6. Stimulated-echo intensities are attenuated as gradient strength is increased from ^{1}H NMR spectra of 1.5/1.5/1/13 mol % DMPC/POPC/DHPC/cholesterol bicelles at $T = 292$ K. As the diffusion time is increased, the diffusion coefficient is decreased due to boundary effect of lipid domains: (a) $\Delta = 50$ ms; (b) $\Delta = 200$ ms; and (c) $\Delta = 700$ ms. Gradient strengths are increased from 0.003 Tm^{-1} to 0.168 Tm^{-1}. Error bars reflect the signal-to-noise ratio of the acyl peak ($\pm 2\sigma$).

to this model, domain formation in the 1.5/1.5/1/13 mol % sample is expected between 270 and 296 K, T_m(POPC) and T_m(DMPC) respectively, and the uniaxial orientation of the domains in the magnetic field would exist between 292 and 296 K (Figure 4). To measure domain formation in the bicelles, we carried out pulsed-field gradient measurements of the lipid self-diffusion constant. In the absence of domains, the diffusion constant should be independent of the diffusion time of the molecules. If domains are present and restrict the lipid diffusion, then the diffusion constant will decrease as the lipid diffusion time increases because the lipid diffusion is confined.[35,40]

3.2.1. Measuring Lipid Diffusion. Figure 5a shows the ^{1}H NMR spectrum of 1.5/1.5/1/13 mol % DMPC/POPC/DHPC/cholesterol bicelles with the choline peak appearing at 3.2 ppm and two acyl chain peaks at 1.2 ppm and 0.8 ppm. The allylic proton peak from POPC appears at 2.0 ppm and WATERGATE has been used to suppress the water peak at 4.7 ppm. For the diffusion measurements, we combined a stimulated-echo pulsed-field bipolar gradient diffusion experiment[48] with water suppression, spinning the sample at the magic angle to obtain well-resolved, isotropic ^{1}H spectra. The acyl peak at 1.2 ppm (marked with an asterisk) was integrated to monitor the lipid signal.

In this experiment, the spin location is encoded by a pair of sine-shaped bipolar gradients of duration δ and amplitude g, bracketing a diffusion time Δ. Diffusion is measured along the direction of the spinning axis with a magic-angle gradient. The intensity of the lipid signal is modulated by the gradient length and amplitude, reflecting the self-diffusion of the lipids. The variation of the signal strength, I, with the experimental parameters can be described by the Stejskal Tanner equation[49]

$$\ln\left(\frac{I}{I_0}\right) = -g^2\gamma^2\delta^2\left(\Delta - \frac{\tau}{2} - \frac{\delta}{8}\right)\cdot D_{\text{meas}} = -k\cdot D_{\text{meas}} \tag{1}$$

where I_0 is the acyl peak integral in the absence of gradients, τ is the spacing of the bipolar gradient pulses, and γ is gyromagnetic ratio for the observed nucleus (in this experiment ^{1}H). The measured self-diffusion constant, D_{meas}, can be extracted from a plot of $\ln(I/I_0)$ versus k (shown in Figure 6). Under the magic angle spinning, the aligning force of the bicelles is lost and the membranes adopt a random distribution of the membrane normal with respect to the magnetic field.[50] Therefore, D_{meas} should be multiplied by 3/2 to compensate for the powder pattern to obtain the apparent lateral diffusion constant, D_{app}.[51]

In the absence of confinement, lipids show classical diffusion in two dimensions, with a diffusion constant that is independent

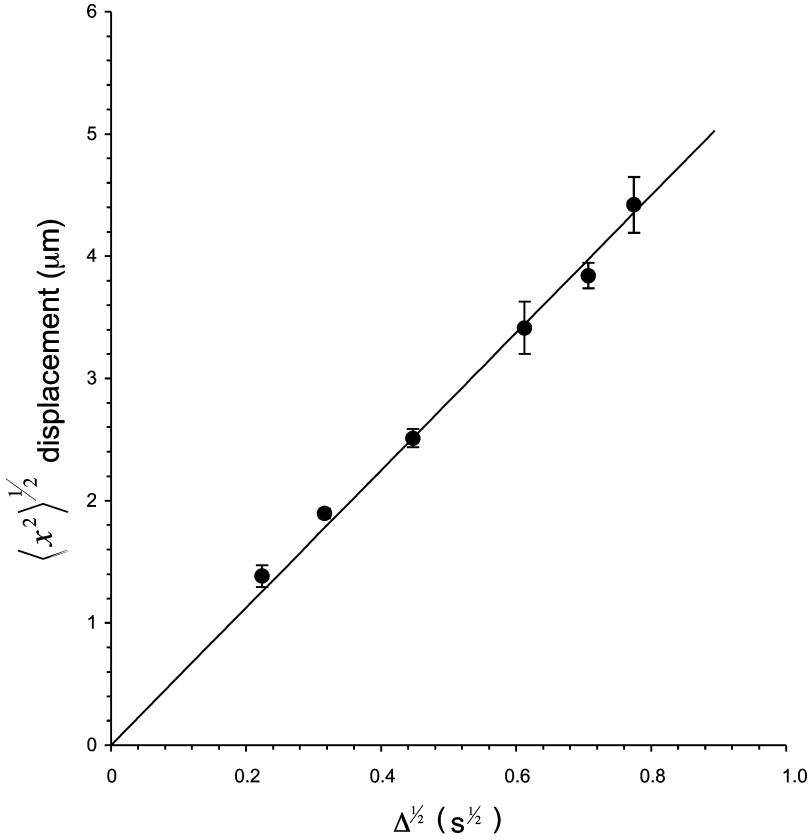

Figure 7. Conventional bicelles (DMPC/DHPC, $q = 3.5$) show a linear relationship between lipid displacement and the square root of diffusion time, consistent with free diffusion. Error bars reflect the fit uncertainty ($\pm 2\sigma$) of the diffusion constant for each point.

of diffusion time. Displacement in free diffusion is described by a Gaussian distribution with the root-mean-square displacement of a lipid increasing with diffusion time, Δ, according to the following equation:

$$\langle x^2 \rangle^{1/2} = \sqrt{4D\Delta} \tag{2}$$

Conventional bicelles containing only DMPC and DHPC are unable to form domains. The long chain lipids in these samples exhibit free diffusion in which the displacement varies linearly with the square root of diffusion time, shown in Figure 7. Each point on this graph represents an apparent diffusion constant measured for a given diffusion time, Δ.

When confined diffusion occurs, the measured diffusion constant decreases with diffusion time, as more molecules encounter the boundary. Figure 6a shows the diffusion measurement of lipids in 1.5/1.5/1/13 mol % bicelles at 292 K, in which the diffusion time, Δ, was 50 ms. As the diffusion time increases to 700 ms (Figure 6a−c), the measured self-diffusion constant is reduced from 4.9×10^{-12} m^2s^{-1} to 1.5×10^{-12} m^2s^{-1}, demonstrating lipid confinement.

In Figure 8, the apparent displacement, $\langle x^2_{app} \rangle^{1/2} = \sqrt{4\bar{D}_{app}\Delta}$, is plotted as a function of the square root of diffusion time for three different temperatures. At 300 K, above the expected miscibility transition, the displacement varies linearly with the square root of diffusion time, indicating free diffusion with no confinement or boundaries as observed in the conventional bicelles (Figure 7). At 295 K, the displacement does not increase linearly with the square root of diffusion time, but rather plateaus at ∼3.0 μm, indicating that the lipids are confined within a micrometer-scale region. At 292 K, the plateau is at ∼2.6 μm, indicating that the areas of confinement decreased with temperature (Figure 8). The changes in diffusion at different temperatures are fully reversible and diffusion measurements made on other samples of the same composition gave results consistent with those presented here.

To extract the true diffusion constant and the domain size, the displacement at 292 and 295 K can be fit to the following equation:[52]

$$\langle x^2 \rangle^{1/2} = r\sin\left(\frac{\sqrt{4D_{true}\Delta}}{r}\right) \tag{3}$$

which reduces to the expression for free diffusion when the domain size, r, is much larger than the displacement (eq 2). The true diffusion constant at 292 K is $4.3 \pm 1.8 \times 10^{-12}$ m^2s^{-1} and $7.3 \pm 2.6 \times 10^{-12}$ m^2s^{-1} at 295 K (Table 2).

The composition of the domains is likely l_d. The size of the domain increases with temperature, consistent with l_d domains, and the domains disappear above the T_m of DMPC. Interestingly, our ^{1}H NMR spectrum of 1.5/1.5/1/13 mol % bicelles shows narrow (∼45 Hz) lipid resonances that increase in intensity from 273 to 310 K as the bicelles align. Previous ^{1}H MAS NMR spectroscopy of similar ternary lipid mixtures (DPPC, DOPC, and cholesterol) showed narrow acyl peaks (∼50 Hz) for l_d domains, similar to our spectra, showing the same basic temperature dependence. However, we observed no signal from the l_o phase, while they observed broad (∼1 kHz) peaks for l_o domains.[53]

This POPC/DMPC bicelle system exhibited micrometer-scale lipid domains, while vesicular systems of POPC/DMPC have shown no domains.[54] In previous work, it was speculated that the asymmetry of the POPC legs decreased its rotational

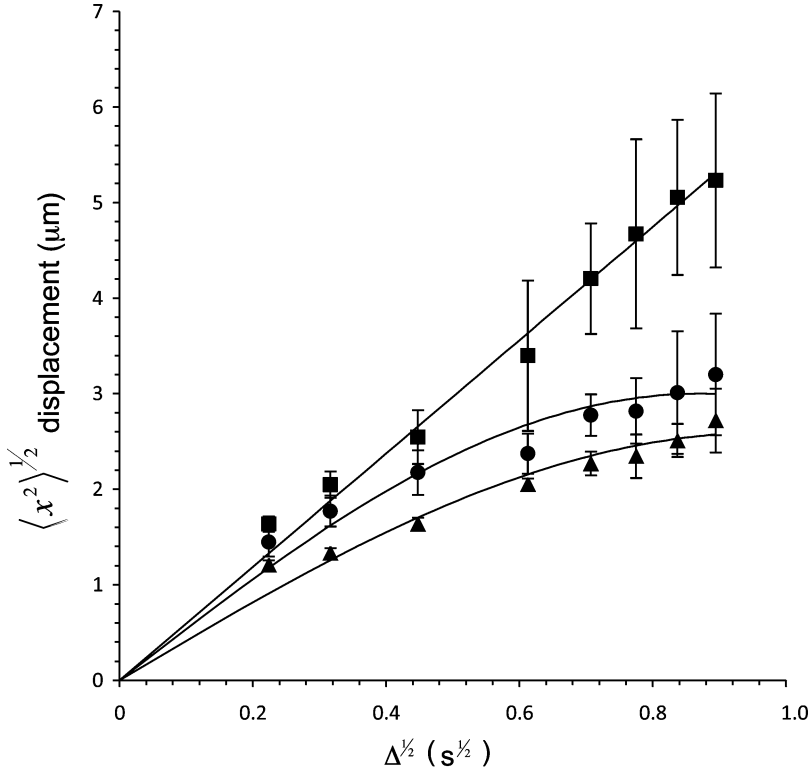

Figure 8. The average displacements in 1.5/1.5/1/chol DMPC/POPC/DHPC unsaturated lipid system with and without rafts as a function of diffusion time at three temperatures. At 300 K (■), the displacement increased as the square root of time, consistent with diffusion. In contrast, at temperatures 295 K (●) and 292 K (▲), the lipid displacements are limited and showed plateaus, indicating confined diffusion within a lipid domain. Error bars reflect the fit uncertainty ($\pm 2\sigma$) of the diffusion constant for each point.

TABLE 2: Diffusion Constants and Domain Sizes in 1.5/1.5/1/13 mol % Bicelle

sample temperature (K)	diffusion constant, D_{true} (10^{-12} m^2s^{-1})	domain size, r (μm)
292	4.3 ± 1.8	2.6 ± 0.4
295	7.3 ± 2.6	3.0 ± 0.3
300	8.8 ± 0.3	

mobility, and hindered formation of the l_o phase.[54] Bicelles exhibit greater lateral and rotational fluidity of the bicelle bilayer than vesicles,[55] apparent in the scaled ^{31}P chemical shift anisotropy of the phosphatidylcholine headgroup, which might affect or favor the formation of domains. The presence of the amphiphile DHPC could play a role in the phase separation directly by partitioning into the bilayer, or the properties of the membrane as a whole simply by stabilizing perforations in the bilayer. Further work characterizing the domain formation in this model membrane, particularly the role of DHPC in domain formation, is underway.

4. Conclusions

In this work, we created a uniaxially aligned membrane containing both saturated and unsaturated lipids, as well as cholesterol, capable of phase separating into lipid domains. Among the various model membranes we created, the 1.5/1.5/1/13 mol % molar ratios of DMPC/POPC/DHPC/cholesterol bicelles showed strong alignment over a large range of temperatures, and exhibited micrometer-scale phase separation into l_o and l_d domains, raising the possibility of structural studies of membrane proteins in rafts and outside of rafts. Structural biology studies of this sort could clarify the molecular action of membrane rafts in cellular biology.

Acknowledgment. We thank Neil Donovan for many helpful discussions and Ad Bax for the conversation sparking this work. We gratefully acknowledge funding support from Eli Lilly and Oak Ridge Associated Universities, as well as funds from the University of Pittsburgh.

References and Notes

(1) Edidin, M. *Annu. Rev. Biophys. Biomol. Struct.* **2003**, *32*, 257.
(2) Lucero, H. A.; Robbins, P. W. *Arch. Biochem. Biophys.* **2004**, *426*, 208.
(3) Caffrey, M. *J. Struct. Biol.* **2003**, *142*, 108.
(4) Marassi, F. M.; Opella, S. J. *Curr. Opin. Struct. Biol.* **1998**, *8*, 640.
(5) Triba, M. N.; Warschawski, D. E.; Devaux, P. F. *Biophys. J.* **2005**, *88*, 1887.
(6) Boesze-Battaglia, K.; Schimmel, R. *J. Exp. Biol.* **1997**, *200*, 2927.
(7) van Meer, G.; Voelker, D. R.; Feigenson, G. W. *Na.t Rev. Mol. Cell. Biol.* **2008**, *9*, 112.
(8) Wassall, S. R.; Brzustowicz, M. R.; Shaikh, S. R.; Cherezov, V.; Caffrey, M.; Stillwell, W. *Chem. Phys. Lipids* **2004**, *132*, 79.
(9) Bakht, O.; Pathak, P.; London, E. 2007, *93*, 4307.
(10) Silvius, J. R. *Biochim. Biophys. Acta, Biomembr.* **2003**, *1610*, 174.
(11) Lee, A. *Biochim. Biophys. Acta* **2004**, *1666*, 62.
(12) Park, S. H.; Opella, S. J. *J. Mol. Biol.* **2005**, *350*, 310.
(13) Turnheim, K.; Gruber, J.; Wachter, C.; Ruiz-Gutierrez, V. *Am. J. Physiol. Cell Physiol.* **1999**, *277*, C83.
(14) Schmidt, D.; Jiang, Q.-X.; MacKinnon, R. *Nature* **2006**, *444*, 775.
(15) van den Brink-van der Laan, E.; Antoinette Killian, J.; de Kruijff, B. *Biochim. Biophys. Acta, Biomembr.* **2004**, *1666*, 275.
(16) Ramamoorthy, A.; Lee, D.-K.; Narasimhaswamy, T.; Nanga, R. P. R. Biochim. Biophys. Acta, Biomembr., In Press, Corrected Proof.
(17) Tokumasu, F.; Jin, A. J.; Feigenson, G. W.; Dvorak, J. A. 2003, *84*, 2609.
(18) Filippov, A.; Oradd, G.; Lindblom, G. 2007, *93*, 3182.
(19) Marcotte, I.; Auger, M. *Conc. Magn. Reson. A* **2005**, *24A*, 17.
(20) Ramamoorthy, A.; Kandasamy, S. K.; Lee, D.-K.; Kidambi, S.; Larson, R. G. *Biochemistry* **2007**, *46*, 965.
(21) Kandasamy, S. K.; Lee, D.-K.; Nanga, R. P. R.; Xu, J.; Santos, J. S.; Larson, R. G.; Ramamoorthy, A. *Biochim. Biophy. Acta, Biomembr.* **2009**, *1788*, 686.

(22) De Angelis, A. A.; Howell, S. C.; Nevzorov, A. A.; Opella, S. J. *J. Am. Chem. Soc.* **2006**, *128*, 12256.
(23) De Angelis, A. A.; Nevzorov, A. A.; Park, S. H.; Howell, S. C.; Mrse, A. A.; Opella, S. J. *J. Am. Chem. Soc.* **2004**, *126*, 15340.
(24) De Angelis, A. A.; Opella, S. J. *Nat. Protocols* **2007**, *2*, 2332.
(25) De Angelis, A. A. *Methods Enzymol.* **2005**, *394*, 350.
(26) Xu, J.; D,rr, U. H. N.; Im, S.-C.; Gan, Z.; Waskell, L.; Ramamoorthy, A. *Angew. Chem., Int. Ed.* **2008**, *47*, 7864.
(27) Minto, R. E.; Adhikari, P. R.; Lorigan, G. A. *Chem. Phys. Lipids* **2004**, *132*, 55.
(28) Triba, M. N.; Devaux, P. F.; Warschawski, D. E. *Biophys. J.* **2006**, *91*, 1357.
(29) Parker, M. A.; King, V.; Howard, K. P. *Biochim. Biophys. Acta, Biomembr.* **2001**, *1514*, 206.
(30) Czerski, L.; Sanders, C. R. *Anal. Biochem.* **2000**, *284*, 327.
(31) Sasaki, H.; Fukuzawa, S.; Kikuchi, J.; Yokoyama, S.; Hirota, H.; Tachibana, K. *Langmuir* **2003**, *19*, 9841.
(32) De Meyer, F. d. r.; Smit, B. *Proc. Natl. Acad. Sci.* **2009**, *106*, 3654.
(33) Lindblom, G.; Johansson, L. B. A.; Arvidson, G. *Biochemistry* **1981**, *20*, 2204.
(34) Edidin, M. *Annu. Rev. Biophys. Bioeng.* **1974**, *3*, 179.
(35) Gaede, H. C.; Gawrisch, K. *Biophys. J.* **2003**, *85*, 1734.
(36) Lindblom, G.; Oradd, G. *Prog. Nucl. Magn. Reson. Spectrosc.* **1994**, *26*, 483.
(37) Filippov, A.; Oradd, G.; Lindblom, G. *Biophys. J.* **2004**, *86*, 891.
(38) Oradd, G.; Westerman, P. W.; Lindblom, G. *Biophys. J.* **2005**, *89*, 315.
(39) Polozov, I. V.; Bezrukov, L.; Gawrisch, K.; Zimmerberg, J. *Nat. Chem. Biol.* **2008**, *4*, 248.
(40) Polozov, I. V.; Gawrisch, K. *Biophys. J.* **2004**, *87*, 1741.
(41) Kadkhodaie, M.; Rivas, O.; Tan, M.; Mohebbi, A.; Shaka, A. J. *J. Magn. Reson.* **1991**, *91*, 437.
(42) Latour, L. L.; Li, L. M.; Sotak, C. H. *J. Magn. Reson., Ser. B* **1993**, *101*, 72.
(43) Tanner, J. E. *J. Chem. Phys.* **1970**, *52*, 2523.
(44) Sanders, C. R.; Schwonek, J. P. *Biochemistry* **1992**, *31*, 8898.
(45) Gennis, R. B. *Biomembranes: Molecular Structure and Function*; Springer-Verlag: New York, 1989.
(46) Yeagle, P. L. *Biochim. Biophys. Acta, Rev. Biomembr.* **1985**, *822*, 267.
(47) London, E. *Curr. Opin. Struct. Biol.* **2002**, *12*, 480.
(48) Cotts, R. M.; Hoch, M. J. R.; Sun, T.; Markert, J. T. *J. Magn. Reson.* **1989**, *83*, 252.
(49) Stejskal, E. O.; Tanner, J. E. *J. Chem. Phys.* **1965**, *42*, 288.
(50) Zandomeneghi, G.; Williamson, P. T. F.; Hunkeler, A.; Meier, B. H. *J. Biomol. NMR* **2003**, *25*, 125.
(51) Pampel, A.; Karger, J.; Michel, D. *Chem. Phys. Lett.* **2003**, *379*, 555.
(52) Gaede, H. C.; Gawrisch, K. *Biophys. J.* **2003**, *85*, 1734.
(53) Polozov, I. V.; Gawrisch, K. *Biophys. J.* **2006**, *90*, 2051.
(54) Veatch, S. L.; Keller, S. L. *Biophys. J.* **2003**, *85*, 3074.
(55) Sanders, C. R.; Prestegard, J. H. *Biophys. J.* **1990**, *58*, 447.

JP100276U